

## Involvement of endoplasmic reticulum stress in a novel Classic Galactosemia model

Tatiana I. Slepak <sup>a</sup>, Manshu Tang <sup>a,b</sup>, Vladlen Z. Slepak <sup>c</sup>, Kent Lai <sup>a,\*</sup>

<sup>a</sup> The Dr. John T. Macdonald Foundation Center for Medical Genetics, Department of Pediatrics, The Leonard M. Miller School of Medicine, University of Miami, P.O. Box 016820 (D-820), Miami, FL 33101, USA

<sup>b</sup> Department of Biochemistry and Molecular Biology, The Leonard M. Miller School of Medicine, University of Miami, Miami, FL 33101, USA

<sup>c</sup> Department of Molecular and Cellular Pharmacology, The Leonard M. Miller School of Medicine, University of Miami, Miami, FL 33101, USA

Received 12 June 2007; accepted 12 June 2007

Available online 20 July 2007

### Abstract

Inherited deficiency of galactose-1-phosphate uridylyltransferase (GALT) activity in humans leads to a potentially lethal disorder called Classic Galactosemia. It is well known that patients often accumulate high levels of galactose metabolites such as galactose-1-phosphate (gal-1-p) in their tissues. However, specific targets of gal-1-p and other accumulated metabolites remain uncertain. In this study, we developed a new model system to study this toxicity using primary fibroblasts derived from galactosemic patients. GALT activity was reconstituted in these primary cells through lentivirus-mediated gene transfer. Gene expression profiling showed that GALT-deficient cells, but not normal cells, responded to galactose challenge by activating a set of genes characteristic of endoplasmic reticulum (ER) stress. Western blot analysis showed that the master regulator of ER stress, BiP, was up-regulated at least threefold in these cells upon galactose challenge. We also found that treatment of these cells with galactose, but not glucose or hexose-free media reduced  $\text{Ca}^{2+}$  mobilization in response to activation of Gq-coupled receptors. To explore whether the muted  $\text{Ca}^{2+}$  mobilization is related to reduced inositol turnover, we discovered that gal-1-p competitively inhibited human inositol monophosphatase (hIMPase1). We hypothesize that galactose intoxication under GALT-deficiency resulted from accumulation of toxic galactose metabolite products, which led to the accumulation of unfolded proteins, altered calcium homeostasis, and subsequently ER stress.

© 2007 Elsevier Inc. All rights reserved.

**Keywords:** Galactosemia; Galactose-1-phosphate; Inositol monophosphatase; Endoplasmic reticulum stress; Unfolded protein response; GRP78

### Introduction

Classic Galactosemia (G/G) is an autosomal recessive, multi-system disorder caused by deleterious mutations of the human galactose-1-phosphate uridylyltransferase (GALT) gene, which results in inability to metabolize galactose [1–3] (Fig. 1). Although a galactose-restricted diet prevents the neonatal lethality of this disorder, many well-treated patients continue to develop debilitating complications such as premature ovarian failure (POF), mental retardation, and some neurological defects [4,5]. The causes of these unsatisfactory outcomes remain unclear. Recent

studies, however, showed that patients placed on a galactose-restricted diet are never truly free of galactose insult, as a significant amount of galactose is found in non-dairy foodstuffs such as vegetables and fruits [6,7]. More importantly, galactose moieties can be produced endogenously from UDP-glucose via the UDP-4-galactose epimerase (GALE) reaction (Fig. 1), and natural turnover of glycoproteins/glycolipids. In fact, using isotopic labeling, Berry et al. elegantly demonstrated that a 50 kg adult male could produce up to 2 g of galactose per day [8,9]. Once the galactose is formed intracellularly, it will be converted to galactose-1-phosphate (gal-1-p) by galactokinase (GALK).

Paradoxically, patients with an inherited deficiency of galactokinase (GALK) do not manifest either the acute toxicity syndrome or chronic complications seen in

\* Corresponding author. Fax: +1 305 243 7255.

E-mail address: [klai@med.miami.edu](mailto:klai@med.miami.edu) (K. Lai).

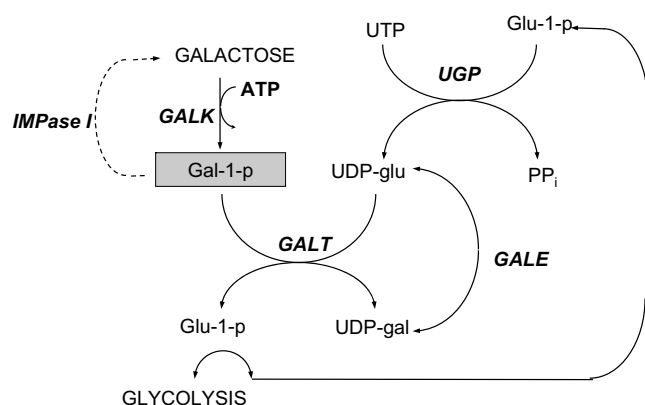


Fig. 1. Schematic representation of galactose metabolic pathway. After entry to cells, galactose is phosphorylated by galactokinase (GALK) to form galactose-1-phosphate (Gal-1-p). In the presence of galactose-1-phosphate uridylyltransferase (GALT), gal-1-p reacts with UDP-glucose to form UDP-galactose (UDP-gal) and glucose-1-phosphate (Glu-1-p). Glucose-1-phosphate formed can either enter glycolysis or react with UTP to yield a new molecule of UDP-glucose in the presence of UDP-glucose pyrophosphorylase (UGP). UDP-galactose can also be produced from UDP-glucose directly by UDP-glucose-4-epimerase (GALE). Gal-1-p can also be dephosphorylated by inositol monophosphatase (IMPase).

galactosemic patients [3]. Since GALK-deficient patients do not accumulate gal-1-p in their tissues [3,10], researchers have long proposed that gal-1-p plays a significant role in the pathogenesis of Classic Galactosemia [11–14]. Yet the *in vivo* targets of this presumably toxic intermediate have never been identified. Concurrently, the lack of overt galactose toxicity in the GALT-knockout mouse model has continued to hamper the efforts to delineate the molecular mechanism of this disease [15–17].

In this study, we developed a novel isogenic human cell model of GALT-deficiency, and showed that galactose challenge of these cells resulted in accumulation of gal-1-p and distinct signs of endoplasmic reticulum (ER) stress. Thus, our findings not only shed light on the pathogenic mechanisms of Classic Galactosemia, but also expanded the contemporary metabolomics model that depicted the fundamental genetic/physical interactions between galactose utilization and other metabolic pathways [18].

## Materials and methods

### Cell lines and culture conditions

Three primary human fibroblasts cell lines derived from galactosemic patients were obtained from Coriell Cell Repositories (Camden, NJ, USA): GM01703, GM01417, and GM00528. All three lines were confirmed by DNA sequencing to be homozygous for the Q188R mutation in the GALT gene, which results in complete loss of enzyme activity [19–21]. For routine maintenance and propagation, the cells were grown in high glucose Dulbecco's minimum Eagle's medium (DMEM) (Gibco 11995-073) supplemented with 10% fetal bovine serum (FBS). Cells beyond passage 30 were not used for experiments and therefore, multiple aliquots of earlier passages were frozen. For experiments with hexose challenge, cells were washed once with phosphate-buffer saline (PBS) and then

transferred to DMEM without glucose and sodium pyruvate (Gibco, 11966-025) supplemented with dialyzed 10% FBS. Glucose or galactose was added when necessary at indicated concentrations.

### Lentiviral vectors and viral infection of fibroblasts

The procedures for the construction of recombinant plasmids and infection of the fibroblasts were described by Follenzi and Naldini [22,23]. The three original plasmids p156RRLsinPPThCMVMCSpre, pMD2.VSVG, and pCMVdR8.74 used in the construction were kindly provided by Dr. Bas Blits (Department of Neurological Surgery, University of Miami Miller School of Medicine). Histidine tagged GALT cDNA was amplified by PCR and sub-cloned into BamHI and NheI sites of the first plasmid. All three plasmids were subsequently transfected to HEK293T cells (ATCC, Manassas, VA, USA). Replication-incompetent virus released into the media was collected and used to infect fibroblasts. The use of lentiviral-based vectors was approved by the Biosafety Committee of the University of Miami Miller School of Medicine (UM Protocol 04-24).

### Western blot analysis

Cells were grown in 100 mm dishes under corresponding conditions, then washed twice with PBS and scraped in 150  $\mu$ l of ice cold hypotonic buffer containing 25 mM Tris-HCl, pH 7.4, 25 mM NaCl, 0.5 mM EDTA and protease inhibitor cocktail (Roche, No. 11 697 498 001). The lysates were passed five times through a 30 gauge needle and centrifuged for 20 min at 16,000g and 4  $^{\circ}$ C. The supernatant was saved as the cytosolic fraction and the pellet was re-suspended in 80  $\mu$ l of RIPA buffer containing 150 mM NaCl, 50 mM Tris-HCl, pH 7.4, 1 mM EDTA, 1% Triton X-100, and protease inhibitors.

Protein concentration was determined using Bio-Rad Dc Protein Assay (Bio-Rad, CA, No. 500-0114). Proteins were separated by SDS gel electrophoresis and analyzed by Western blot as described previously [21]. Anti-EGFR, anti-IP<sub>3</sub> receptor, anti-GRP78/BiP, and anti- $\beta$ -actin antibodies were purchased from Santa Cruz Inc., CA.

### GALT activity and gal-1-p assay

Assays for GALT activity and gal-1-p in the fibroblast cell lines were performed using the published methods [13,21].

### DNA microarray analysis

DNA microarray analysis was performed at the DNA Microarray Core Facility at The University of Miami Miller School of Medicine (<http://www.biomed.miami.edu/arrays/>). Briefly, total RNA from the samples was isolated and purified using TRI Reagent (Molecular Research Center No. TRI-118) and RNeasy Mini Kit (Qiagen, No. 74106). Total RNA yield was determined spectrophotometrically. RNA quality was assessed using an Agilent 2100 Bioanalyzer and its software. Labeling, and hybridization to Agilent Whole Human Genome Arrays (Agilent No. G4410A), were performed using established protocols. The microarrays were scanned at 10 micron resolution using a GenePix 4000A scanner (Axon Instruments at Molecular Devices) and the resulting images were analyzed with the software package GenePix Pro 5.1 (Axon Instruments at Molecular Devices). Data extracted from the images were transferred to the software package Acuity 4.0 (Axon Instruments) for normalization and statistical analysis. Each array was normalized for signal intensities across the whole array and locally, using Lowess normalization.

To identify significantly expressed genes across all replicate arrays, one-class SAM (Significant Analysis of Microarray, <http://www-stat.stanford.edu/~tibs/SAM>) analysis [24] was used with the FDR (False Discovery Rate) set at 1%. All primary microarray data were submitted to the public database at the GEO web site (<http://www.ncbi.nih.gov/>

geo). Selected genes were classified according to the Gene Ontology category “biological process” using Onto-Express (<http://vortex.cs.wayne.edu/Projects.html>) [25–27].

### Quantitative real-time PCR

Fibroblasts cultured in glucose medium were challenged with galactose as indicated in text, and RNA was extracted with RNA easy kit (Qiagen) according to the manufacturer’s recommendations. The synthesis of the first-strand cDNA was conducted using Reverse Transcriptase (Roche) with oligo(dT)18 primer (New England BioLabs) in a total volume of 20  $\mu$ l containing 5  $\mu$ g total RNA. Real-time PCR was performed with TAQuarte GREEN Real-Time PCR Master Mix (Epicenter Biotechnologies) in Eppendorf Mastercycler, and the results were analyzed with Eppendorf RealPlex software. The protocol used was: 2 min at 94 °C followed by 40 cycles of 15 s at 94 °C for denaturing, 20 s at 56 °C for annealing, and 20 s at 72 °C for extension. We used GAPDH gene as an internal control. Target gene sequences were amplified with different sets of primers as follows:

|              |   |
|--------------|---|
| Calreticulin | 5'-CGCTGGCTACCGTCTATTTC-3'<br>3'-CGTGCAGAGATGGCATAGAA-5'  |
| CHOP         | 5'-GCGCATGAAGGAGAAAGAAC-3'<br>3'-CCAATTGTTTCATGCTTGGTG-5' |
| EGFR         | 5'-ACATGTTCGATGGACTCCAGAAC<br>5'-AATTACGGGGACACTTCTTCAC   |
| GRP94        | 5'-TGGGAAGAGGTTCCAGAATG-3'<br>3'-GTTGCCAGACCATCCGTACT-5'  |
| GAPDH        | 5'-GAGTCAACGGATTGGTCTCGT-3'<br>3'-TTGATTTTGGAGGGATCTCG-5' |
| GRP78/BiP    | 5'-TAGCGTATGGTGCTGCTGTC-3'<br>3'-TTTGTCAGGGGTCTTTCACC-5'  |

The relative amounts of the target gene, standardized against the amount of GAPDH were expressed as  $\Delta C_t = C_{t(\text{target})} - C_{t(\text{GAPDH})}$ , where  $C_t$  is the cycle number at the threshold of the early exponential phase. The ratio of the same target gene in different samples was expressed as  $2^{\Delta C_{t1} - \Delta C_{t2}}$ , where  $\Delta C_{t1}$  represents the  $\Delta C_t$  value for sample 1 and  $\Delta C_{t2}$  represents the  $\Delta C_t$  value for sample 2. Each sample was repeated three times and the mean value and standard deviation were calculated.

### Competition studies

Human inositol monophosphatase I (hIMPaseI) cDNA clone was purchased from Open Biosystems. cDNA was amplified by PCR and subcloned into the bacterial expression vector pET15b (Novagen). The hIMPase was over-expressed in *Escherichia coli* strain BL21(DE3) (Novagen) and purified using nickel-affinity chromatography (Ni-NTA, Qiagen, No. 1004493). Inositol monophosphatase activity in the presence of varying amounts of gal-1-p was measured by the amount of inositol produced using the method described by Dolhofer and Wieland [28].

### Ex vivo $\text{Ca}^{2+}$ imaging

The corresponding cell lines were grown on glass coverslips in the presence/absence of 0.1% galactose at a confluency of about 70%. The cells were loaded with 5  $\mu$ M Fura-2AM (Molecular Probe, Invitrogen, CA, No. F-1201) at 37 °C in a CO<sub>2</sub> incubator for 45 min in HBSS buffer (25 mM Hepes, pH 7.4, 140 mM NaCl, 5 mM KCl, 2 mM CaCl<sub>2</sub>, 1.2 mM MgSO<sub>4</sub>, 1.2 mM KH<sub>2</sub>PO<sub>4</sub>, and 6 mM galactose), supplemented with 2% FBS, following a 30 min incubation in serum free HBSS buffer without Fura-2AM in the same conditions. The cells were placed in a flow chamber mounted on the inverted fluorescent microscope stage.  $\text{Ca}^{2+}$ -free HBSS buffer (25 mM Hepes, pH 7.4, 140 mM NaCl, 5 mM KCl, 1 mM EGTA, 1.2 mM MgSO<sub>4</sub>, 1.2 mM KH<sub>2</sub>PO<sub>4</sub>, and 6 mM galactose) was used

to wash the cells and deliver a G-protein coupled receptor agonist. The cells were excited at two wavelengths (340 and 380 nm), and the 340/380 ratio was recorded at 20 $\times$  magnification. A  $\text{Ca}^{2+}$  calibration kit (Cat No. F6774, Invitrogen, CA) was used to convert 340/380 ratio values to the concentration of free  $\text{Ca}^{2+}$ . The data were analyzed using the Meta-Fluor software package (Molecular Devices).

## Results

### Reconstitution of GALT activity in GALT-deficient primary fibroblasts prevented galactose toxicity

The lack of explicit galactose toxicity in the GALT-knockout mouse model [15–17] has prompted us to focus on cell models of human origin. In this study, we examined how GALT-deficient and GALT-positive cells behave differently in the presence of galactose. To rule out variation in genetic background between cells derived from healthy and galactosemic individuals, we reconstituted GALT enzyme activity in the fibroblasts derived from the same galactosemic patients using a lentiviral vector expressing the GALT cDNA (pLenti-GALT). The GALT-reconstituted cells therefore serve as isogenic, “normal” control for the GALT-deficient patient cells, which have no detectable GALT activity (Fig. 2a). To control for the infection procedure, we infected the GALT-deficient cells with another lentiviral vector expressing the green fluorescent protein (GFP) (pLenti-GFP). The resulting cells remained GALT-deficient (Fig. 2a). Primary fibroblasts derived from three unrelated galactosemic patients were chosen for this study.

We subjected GALT-deficient (G/G) fibroblasts infected with either pLenti-GFP or pLenti-GALT, to three different growth conditions: (i) hexose-free DMEM with 10% dialyzed FBS, (ii) the same medium with 0.1% glucose, and (iii) the same medium with 0.1% galactose as the main energy source. The hexose-free medium was our control for the potential effects of glucose starvation. We used 0.1% galactose alone to exclude any confounding effects from other energy sources. Our measurements showed that exposure to 0.1% galactose resulted in the accumulation of 1.3 mM gal-1-p in GALT-deficient fibroblasts, which is similar to the concentration of erythrocyte gal-1-p in untreated galactosemic patients [1,3].

We found that all fibroblasts grew normally in the presence of 0.1% glucose. In the hexose-free medium, all fibroblasts rounded up and detached from plate surface by day 3 (Fig. 2b). If cells were cultured further for 2–3 more days, no viable cells remained. In 0.1% galactose medium, GALT-deficient cells (*i.e.*, cells infected with pLenti-GFP) also began to perish by day 3 (panel E, Fig. 2b). In contrast, normal cells and G/G cells reconstituted with GALT continue to grow (panels D and F, Fig. 2b). To investigate if different mechanism(s) account for cell death in hexose-free and galactose containing media, we studied gene expression profiles in our cells in hexose-free and galactose medium.

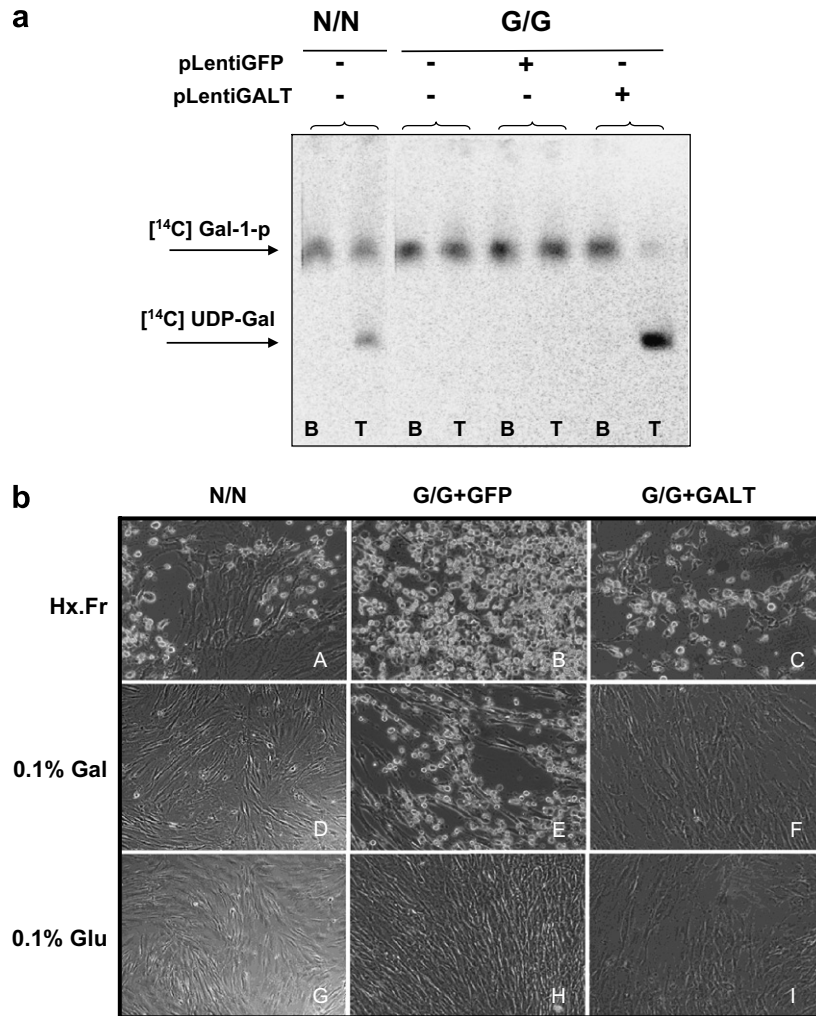


Fig. 2. Reconstitution of GALT activity in GALT-deficient fibroblasts. (a) Enzymatic assay for GALT activity for normal (N/N) and galactosemic (G/G) cells. Infection with lentivirus harboring either GFP (pLenti-GFP) or GALT (pLenti-GALT) is indicated. Only cells expressing GALT activity converted [<sup>14</sup>C]-gal-1-p to [<sup>14</sup>C]-UDP-galactose (shown by arrows), which were separated by DEAE-TLC as shown in the test (T) lanes. The blank (B) lanes represented control reactions in which one of the two substrates of GALT, UDP-glucose, was omitted. (b) Fibroblasts derived from galactosemic patients (G/G) and normal controls (N/N) were grown in either hexose-free DMEM (Hx.Fr.) or same media substituted with 0.1% galactose (0.1% gal) or 0.1% glucose (0.1% glu). G/G cells were infected with either pLenti-GFP (G/G+GFP) or pLenti-GALT (G/G+GALT) viruses (see text). Phase contrast images are taken on the third day of culture.

#### Galactose challenge of GALT-deficient fibroblasts triggers ER stress

We used 60-mer oligonucleotide-based whole genome microarrays to determine how GALT-deficient and GALT-positive cells behave differently in the presence of galactose. Competitive hybridization experiments were performed, in duplicate, on three different GALT-deficient cell lines and their GALT-reconstituted counterparts. Using a total of six data sets, we conducted pair wise comparisons and focused on genes whose expression level was changed over twofold in a similar manner in all six comparisons (Table 1).

To control for the effect of starvation, we performed identical hybridization experiments on the respective cell lines grown in hexose-free medium. The changes seen in

this medium were strikingly different from those where cells were grown in the presence of galactose, and very few overlapping genes were detected (see [Supplemental material](#)). These results indicated that the molecular mechanisms underlying cell death triggered by galactose toxicity are distinct from the mechanism activated by starvation.

We noticed that many genes involved in unfolded protein response (UPR) were up-regulated in all three galactose-challenged, GALT-deficient fibroblasts (*i.e.*, G/G cells that were infected with pLenti-GFP). In mammalian cells, the UPR signal transduction pathway is designed to cope with ER stress, which is caused by accumulation of mis-folded proteins in the ER [29–31]. We observed an increased expression of transcriptional activators such as CHOP, ATF4, ATF3, which up-regulate genes that encode ER resident protein chaperones (*e.g.*, GRP78/BiP, GRP94,



Table 1  
Genes up-regulated in GALT-deficient fibroblasts under galactose challenge

| Gene symbol   | Gene name/function   | Mean (stats) | SD (stats) | CV (stats) |
|---|--|--------------|------------|------------|
| <i>Chaperones, HSP70 class</i>                                      |  |              |            |            |
| BiP   | Heat shock 70 kDa protein 5 (glucose-regulated protein, 78 kDa)                | 10.66        | 2.72       | 42.32      |
| HSPA9B  | Heat shock 70 kDa protein 9B (mortalin-2)                                      | 2.85         | 1.15       | 13.07      |
| STCH  | Stress 70 protein chaperone, microsome-associated, 60 kDa                      | 4.11         | 1.23       | 14.46      |
| <i>Chaperones, HSP90 class</i>                                      |  |              |            |            |
| GRP94   | Human endoplasmic precursor (94 kDa glucose-regulated protein) (GRP94)         | 5.77         | 2.21       | 45.15      |
| <i>Chaperones, DNA-J-like, HSP40 class</i>                          |  |              |            |            |
| DNAJC3  | DnaJ (Hsp40) homolog, subfamily C, member 3                                    | 4.36         | 1.49       | 27.32      |
| DNAJB9  | DnaJ (Hsp40) homolog, subfamily B, member 9                                    | 5.65         | 1.51       | 23.90      |
| DNAJB11   | DnaJ (Hsp40) homolog, subfamily B, member 11                                   | 4.58         | 1.47       | 25.47      |
| DNAJC10   | DnaJ (Hsp40) homolog, subfamily C, member 10                                   | 3.24         | 1.37       | 26.75      |
| DNAJC1  | DnaJ (Hsp40) homolog, subfamily C, member 1                                    | 2.07         | 1.03       | 3.45       |
| <i>Lectins</i>  |  |              |            |            |
| CANX  | Calnexin   | 3.13         | 1.33       | 24.68      |
| CALR  | Calreticulin   | 4.37         | 1.40       | 22.70      |
| <i>Foldases, subclass disulfide isomerases</i>                      |  |              |            |            |
| PDA3  | Human protein disulfide isomerase A3 precursor (disulfide isomerase ER-60)     | 3.24         | 1.49       | 33.85      |
| PDA4  | Human protein disulfide isomerase A4 precursor (protein ERp-72) (ERp72)        | 4.91         | 1.79       | 36.53      |
| TXNDC4  | Thioredoxin domain containing 4 (endoplasmic reticulum)                        | 2.75         | 1.17       | 15.14      |
| TXNDC7  | Thioredoxin domain containing 7 (protein disulfide isomerase)                  | 3.47         | 1.66       | 40.74      |
| ERO1L   | ERO1-like  | 2.51         | 1.22       | 21.89      |
| ERO1-like beta ( <i>S. cerevisiae</i> )                             | ERO1-like beta   | 2.16         | 1.09       | 12.00      |
| ERP44   | Erp44 protein ( <i>Homo sapiens</i> ), complete                                | 2.67         | 1.14       | 13.52      |
| ERP70   | Protein disulfide isomerase related protein (calcium-binding protein)          | 5.28         | 1.91       | 38.83      |
| <i>Transcriptional activation factors for ER stress response</i>    |  |              |            |            |
| CHOP  | DNA-damage-inducible transcript 3  | 5.65         | 1.65       | 28.96      |
| ATF3  | Activating transcription factor 3  | 3.03         | 1.22       | 18.25      |
| ATF4  | Activating transcription factor 4 (tax-responsive enhancer element B67)        | 2.47         | 1.16       | 11.20      |
| GADD45A   | Growth arrest and DNA-damage-inducible, $\alpha$                               | 2.84         | 1.23       | 19.45      |
| XPB1  | X-box binding protein 1  | 2.72         | 1.21       | 18.93      |
| <i>ER associated protein degradation</i>                            |  |              |            |            |
| HRD1  | Synovial apoptosis inhibitor 1, synoviolin                                     | 3.04         | 1.14       | 11.76      |
| EDEM1   | ER degradation enhancer, mannosidase $\alpha$ -like 1                          | 4.08         | 1.38       | 22.83      |
| HERPUD1   | Homocysteine-inducible, endoplasmic reticulum stress-inducible, ubiquitin-like | 5.98         | 1.66       | 28.24      |
| DER1  | ER-associated protease   | 2.07         | 1.24       | 20.00      |
| <i>Other ER proteins/chaperones associated with stress response</i> |  |              |            |            |
| TRA1  | Tumor rejection antigen (gp96) 1   | 5.68         | 2.16       | 44.22      |
| HYOU1   | Hypoxia up-regulated 1   | 7.98         | 1.61       | 22.83      |
| GRP58   | Glucose regulated protein, 58 kDa  | 3.65         | 1.45       | 28.53      |
| SERP1   | Stress-associated endoplasmic reticulum protein 1                              | 2.45         | 1.13       | 13.85      |
| SEL1L   | sel-1 suppressor of lin-12-like ( <i>C. elegans</i> )                          | 4.89         | 1.56       | 28.11      |
| ALG2  | Asparagine-linked glycosylation 2 homolog ( $\alpha$ -1,3-mannosyltransferase) | 2.37         | 1.12       | 13.36      |
| GALNACT-2   | Chondroitin sulfate GalNAcT-2  | 2.36         | 1.17       | 18.58      |
| SEC63   | SEC63-like ( <i>S. cerevisiae</i> )  | 2.75         | 1.19       | 16.98      |
| GLRX  | Glutaredoxin (thioltransferase)  | 3.09         | 1.14       | 11.95      |

Mean and SD (standard deviation) values represented fold changes of gene expression in GALT-deficient versus GALT-reconstituted fibroblasts, CV (coefficient of variation) are in %.

GRP58, HYOU1), lectins (CANX, CALR), and foldases (e.g., ERP44, ERO1L, ERP70) (Table 1). The elevation of protein chaperones, lectins, and foldases is typical for cells under ER stress, as these proteins function to enhance the folding capacity of the ER [30,32]. It is known that if such molecular responses are not sufficient to cope with

the stress, the cells attempt to eliminate mis-folded proteins via up-regulation of ER resident proteases such as EDEM1 and DER1 (Table 1) [33–35].

Importantly, there was no difference between global gene expression profiles of the pLenti-GFP- and pLenti-GALT-infected cells if they were cultured in glucose, except

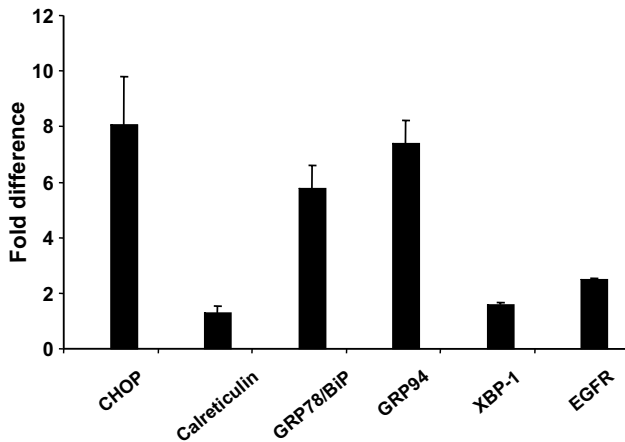


Fig. 3. Verification of expression microarray data by quantitative real-time PCR. Quantitative real-time PCR was performed on selected genes in GALT-deficient and GALT-positive cells challenged with 0.1% galactose. The graph represents the fold-differences in expression level of the selected genes in the GALT-deficient cells in 0.1% galactose (error bars represents one standard deviation).

for the up-regulation of GALT gene in the latter cells (data not shown). Thus, over-expression of GALT alone did not appear to have a significant effect on global gene expression, nor did it cause stress to the cells. This is also supported by the observation that patients with the *Los Angeles* variant of GALT gene have higher-than-normal GALT activity, but no adverse symptoms [36].

To confirm the gene expression array data, we performed real-time, quantitative RT-PCR of the following genes: CHOP, calreticulin, GRP78/BiP, GRP94, and XBP-1. GAPDH was used as an internal control. As seen in Fig. 3, the significantly higher expression levels of these ER stress related genes observed in expression array experiment in the galactose-intoxicated GALT-deficient cells were confirmed by real-time quantitative PCR. Furthermore, Western blot analysis showed that the master ER stress sensor protein, GRP78/BiP was up-regulated in the GALT-deficient cells cultured in galactose (Fig. 4a). However, GRP78/BiP has also been previously shown to elevate during starvation [37,38]. We tested whether starvation-mediated up-regulation of GRP78/BiP also occurred in our cells. Indeed we found that this protein was up-regulated in hexose-free medium (Fig. 4a). To test whether up-regulation of this protein in galactose was due to starvation, we cultured G/G cells in the mixture of galactose and glucose. We found that the level of GRP78/BiP protein in the mixture of sugars was comparable to that in galactose alone, indicating that the mechanism inducing up-regulation of GRP78/BiP in the presence of galactose was distinct from glucose starvation. Additionally, the up-regulation of GRP78/BiP protein was proportional to the amount of galactose present in the media (Fig. 4b). Taken together, these results demonstrate that reconstitution of GALT activity in the GALT-deficient cells rescues them from galactose-induced ER stress.

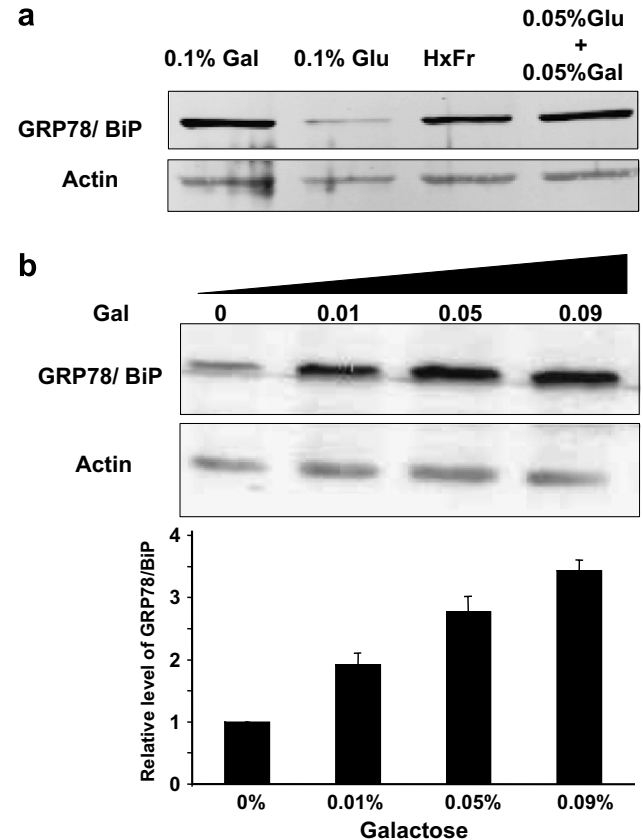


Fig. 4. Up-regulation of GRP78/BiP in GALT-deficient cells under galactose challenge. (a) Western blot analysis of GALT-deficient cells grown in 0.1% galactose (Gal); 0.1% glucose (Glu), hexose-free (HxFr) and 0.05% glucose + 0.05% galactose (Glu + Gal), respectively stained with anti-GRP78/BiP and anti-actin antibodies. (b) Western blot analysis of GALT-deficient cells grown in 0.005% glucose supplemented with increasing concentrations of galactose (Gal) shown in percentage above each lane. The blot was stained with anti-GRP78/BiP and anti-actin antibodies. The protein abundance level of GRP78/BiP was normalized to that of actin in each sample. The relative amount of GRP78/BiP protein in each sample was then further normalized to the sample with 0% galactose, which was arbitrarily assigned as 1.

#### ER stress response to galactose toxicity affects expression of epidermal growth factor receptor (EGFR)

We noted that GALT-deficient cells grow much slower than normal, even in glucose-containing medium. Since the growth of fibroblasts is dependent on the expression level of EGFR, we compared the levels of this protein in several GALT-deficient cell lines grown in the presence of glucose or galactose. Fig. 5 shows that the abundance of this receptor was markedly reduced in the GALT-deficient cells when they were shifted to 0.1% galactose for 48 h (compare lanes 4, 5 and 10, 11). This change of EGFR protein level was not observed for normal fibroblasts (compare lanes 1–3 and 7–9 in Fig. 5).

Reconstitution of GALT activity in the GALT-deficient fibroblasts resulted in a restoration of EGFR protein to the level comparable to that in glucose medium (lane 12, Fig. 5), confirming the role of normal GALT function on

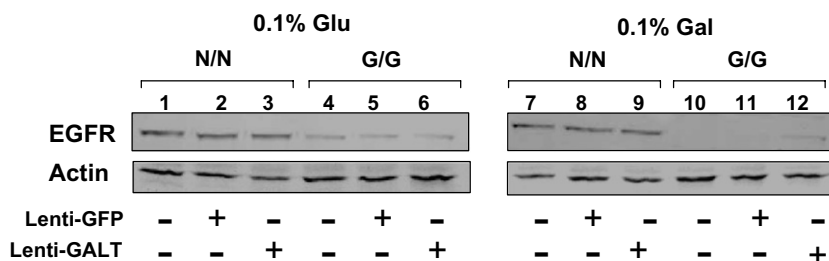


Fig. 5. Expression of EGFR is GALT-dependent under galactose toxicity. Normal (N/N) and galactosemic (G/G) cells were grown in the presence of 0.1% glucose (0.1% glu) or 0.1% galactose (0.1% gal) with anti-EGFR antibody. Cells were infected with lentiviral vectors expressing GFP (pLenti-GFP) or GALT (pLenti-GALT) as indicated. Cell lysates were analyzed by Western blot analysis with anti-EGFR antibody. Staining with anti-actin antibody was used as loading control.

the abundance of EGFR. To determine if reduced EGFR protein abundance in the GALT-deficient cells was caused by reduced EGFR RNA level, we performed quantitative real-time PCR. Interestingly, the transfer of the GALT-deficient cells (either non-infected or infected with pLenti-GFP) to galactose medium did not produce any reduction in EGFR mRNA level (Fig. 3). This data suggested that lower level of EGFR protein in the galactose-intoxicated cells was likely resulted from a change in EGFR protein synthesis or turnover, both of these processes are linked to the functional state of the ER.

ER stress is initiated mainly by exposure to conditions that cause accumulation of mis-folded proteins. Perturbation of calcium homeostasis in the ER is known to be one such initiator [32]. Hence, we tested if any such perturbations occur in the galactose-intoxicated cells.

#### *Ca<sup>2+</sup> homeostasis is altered in galactose-intoxicated cells*

We analyzed calcium release by monitoring changes in free Ca<sup>2+</sup> cytoplasmic levels in response to 25 nM bradykinin (BK). Stimulation of G<sub>q</sub>-coupled BK receptor causes Ca<sup>2+</sup> release from the ER storage *via* activation of phospholipase C and IP<sub>3</sub> release [39].

As shown in Fig. 6a, free Ca<sup>2+</sup> release into the cytoplasm upon BK stimulation is significantly diminished in galactosemic cells cultured in galactose. Restoration of GALT activity increases the amount of Ca<sup>2+</sup> released similar to the levels seen in normal cells. No difference in Ca<sup>2+</sup> response was observed when cells were cultured in hexose-free medium (Fig. 6b), indicating that reduced Ca<sup>2+</sup> release is specific to galactose toxicity and does not result from starvation. Thus, our data strongly showed that galactose toxicity in GALT-deficient cells specifically perturbs Ca<sup>2+</sup> release through IP<sub>3</sub> receptor-mediated pathway.

To determine if the muted Ca<sup>2+</sup> response was related to changes in IP<sub>3</sub> receptor in the GALT-deficient cells, we tested if galactose challenge resulted in reduced abundance of IP<sub>3</sub> receptor (Fig. 6c). The level of IP<sub>3</sub> receptor was unchanged. These results suggested that the low Ca<sup>2+</sup> release is either a result of compromised Ca<sup>2+</sup> storage in the ER or diminished IP<sub>3</sub> release from reduced phosphatidylinositol diphosphate (PIP<sub>2</sub>).

#### *Gal-1-p is a competitive inhibitor of inositol monophosphatase (IMPase)*

It was previously shown that IMPase can dephosphorylate gal-1-p *in vitro* [40]. Furthermore, Bhat hypothesized that gal-1-p can modulate the IMPase activity [11]. We investigated the effect of gal-1-p on IMPase-mediated hydrolysis of inositol-1-phosphate (I-1-p). Our kinetic analysis demonstrated that gal-1-p competitively inhibited human IMPase1 by increasing its  $K_M$  for I-1-p from  $320 \pm 50 \mu\text{M}$  to  $980 \pm 70 \mu\text{M}$  without changing the  $V_{\text{max}}$  (Fig. 7). The amount of competing gal-1-p in our reactions was comparable to that found in galactosemic patients. Thus, gal-1-p can inhibit IMPase *in vivo*, potentially affecting inositol metabolism.

#### Discussion

Despite the advances made in the biochemical characterization of Classic Galactosemia and the molecular/structural biology of the human GALT gene in the past four decades [3,20,41,42], the pathogenesis of this disease remains largely unknown and the long-term outcome continues to be poor [4,5,43]. Faced with the lack of overt galactose toxicity in the GALT-knockout mouse model [15–17], researchers nonetheless proposed that galactose-1-phosphate (gal-1-p) plays a major role in causing acute toxicity syndrome and chronic complications [44–46]. It has been recognized that patients with inherited deficiency of galactokinase (GALK) do not accumulate gal-1-p in their tissues, nor manifest either the acute toxicity syndrome or chronic complications seen in the GALT-deficient patients [3,10,47,48]. Yet the *in vivo* toxicity target(s) of gal-1-p have been elusive. It has also been suggested that galactose challenge of human GALT-deficient cells resulted in “metabolic stress” [3], although the molecular nature of the stress response has not been characterized.

In this study, we developed and investigated a novel human isogenic cell model based on primary human GALT-deficient fibroblasts. We showed, for the first time, that galactose challenge of these cells resulted in up-regulation of genes characteristic of ER stress (Table 1 and Figs. 3, 4). We demonstrated that galactose challenge resulted in

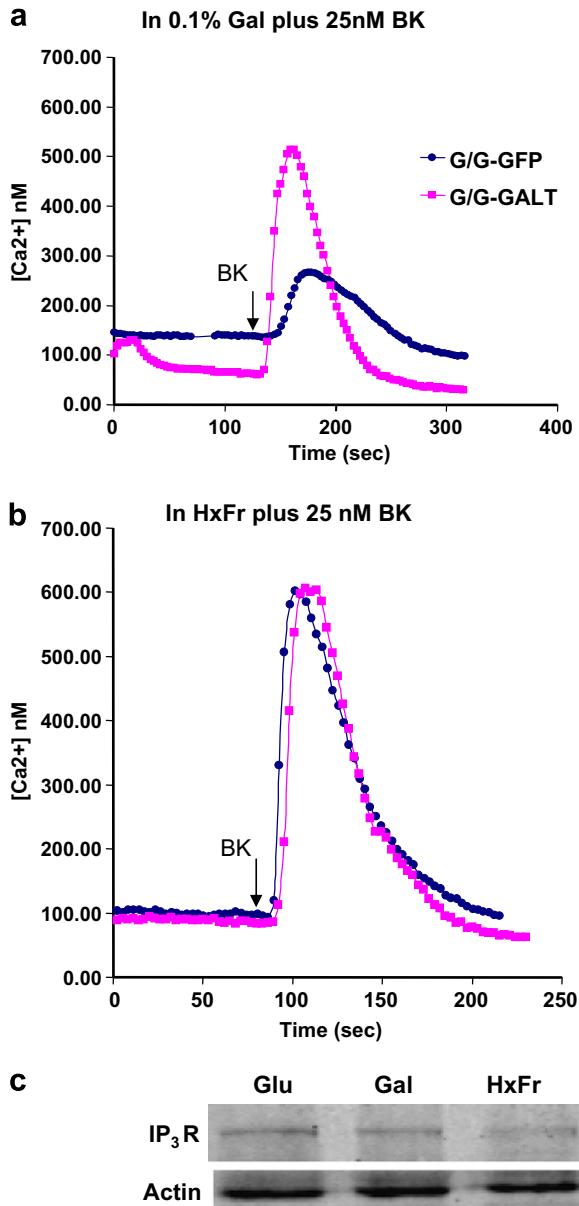


Fig. 6. The effect of GALT-deficiency on agonist-induced free  $\text{Ca}^{2+}$  release.  $\text{Ca}^{2+}$  release was recorded using ratiometric Fura-2 dye as described in Materials and methods. Each trace represents an average of recordings from 20 to 40 individual cells in the field of a microscope. The time of addition of the 25 nM bradykinin—BK is marked by arrow. Galactosemic (G/G) cells were infected with lentivirus expressing either GFP (G/G-GFP) (blue line) or GALT (G/G-GALT) (magenta line). (a) Cells were grown in hexose-free DMEM supplemented with 10% dialyzed FBS and 0.1% galactose. (b) Cells were grown in hexose-free DMEM supplemented with 10% dialyzed FBS. (c) Western blot analysis for  $\text{IP}_3$  receptor ( $\text{IP}_3\text{R}$ ) and actin in GALT-deficient cells cultured in hexose-free DMEM (HxFr), or same media supplemented with 0.1% glucose (Glu), 0.1% galactose (Gal).

ER stress rather than starvation by showing that galactose causes up-regulation of ER stress marker BiP even in the presence of glucose, which rules out the effect of starvation (Fig. 4).

Our results shown here also concur with our earlier report on environmental stress response manifested in a

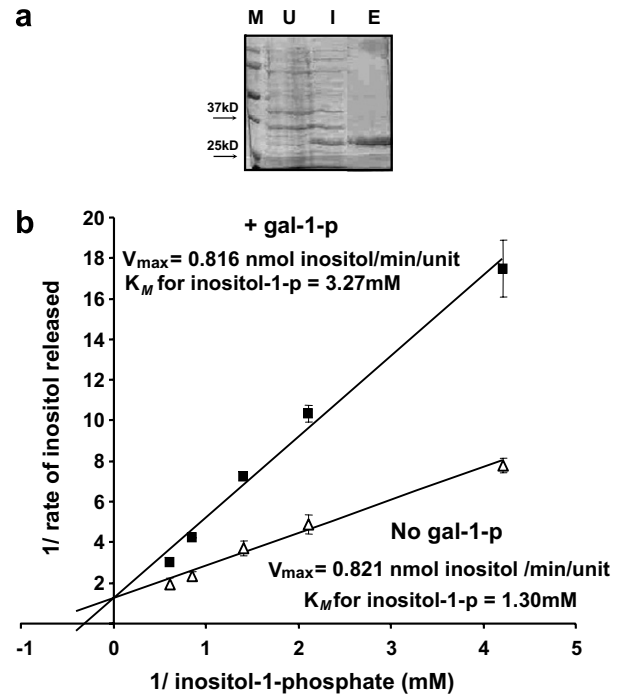


Fig. 7. Competitive inhibition of hIMPase1 by excess gal-1-p. (a) Purification of recombinant human IMPase1. Lanes on SDS-PAGE are as follows: M, molecular weight markers; U, un-induced bacteria crude extract; I, induced bacteria crude extract; E,  $\text{Ni}^{2+}$ -NTA eluate (induced). (b) Lineweaver–Burke plot shows the variation of reaction rates of hIMPase in the presence (solid squares) and absence (clear triangles) of 50 M excess of gal-1-p. Each data point represents the mean of three separate experiments.

GALT-deficient yeast model grown in the presence of galactose [49]. In that study, we discovered that addition of galactose to GALT-deficient yeast, but not GALK-deficient yeast, resulted in cessation of growth and over-expression of genes characteristic of unfolded protein response (UPR) [49]. Thus, we may infer from the yeast study that the ER stress manifested in the galactose-intoxicated fibroblasts was also caused by accumulation of gal-1-p in these cells. But what are the potential toxicity targets of gal-1-p in these cell models?

Previously, we showed that galactose-1-phosphate competitively inhibited UDP-glucose pyrophosphorylase, leading to 66% reduction in UDP-glucose/galactose contents in GALT-deficient cells under galactose challenge [13]. Since UDP-glucose/galactose are crucial glycosyl donors, their deficiencies in these cells will undoubtedly impair protein glycosylation reactions [50], and could in turn trigger ER stress [30,31,50]. Indeed, aberrant glycosylation of glycoproteins and glycolipids have been widely reported in patients with Classic Galactosemia [13,51–55]. The reduction of EGFR, a heavily glycosylated protein with 11 *N*-linked glycosylation sites in the GALT-deficient cells observed in this study is likely to be resulted from impaired protein glycosylation, which would have initiated ER stress in this case. At the same time, ER stress evoked in this case might have led to reduced translation of EGFR mRNA



and/or increased degradation of EGFR protein through ER stress associated degradation (ERAD) (Table 1) [50,56], further diminishing the abundance of this membrane protein (Fig. 5).

In addition to aberrant protein glycosylation, we also examined whether perturbed calcium homeostasis might play a role in inducing ER stress in the galactose-intoxicated cells (Fig. 6). After the discovery that bovine inositol monophosphatase recognizes gal-1-p as a substrate [40], Bhat and other investigators have proposed that gal-1-p accumulated in galactosemic patients may interfere with inositol turnover, which will have significant implications in calcium homeostasis [11]. In this study, we found diminished G protein coupled receptor (GPCR)-mediated  $\text{Ca}^{2+}$  release in cells (Fig. 6) and confirmed that gal-1-p accumulation inhibits human inositol monophosphatase (Fig. 7). We therefore propose that gal-1-p accumulation can indeed cause inositol depletion as shown in other similar studies [57,58]. This in turn results in deficiency of phosphatidylinositides [59], and subsequently, reduction in  $\text{IP}_3$  level and  $\text{Ca}^{2+}$  release from the ER. Diminished  $\text{G}_q$  receptor-mediated calcium release in the galactose-intoxicated cells lent some support to this hypothesis (Fig. 6). However, a more thorough measurement of inositol and phosphatidylinositides contents in these cells in the future are necessary to further substantiate this model.

In conclusion, our studies provide evidence in support of a new hypothesis that galactose intoxication is associated with ER stress. Since our experiments were performed on primary human GALT-deficient fibroblasts, these findings are of relevance to patient phenotypes. For instance, it is tempting to speculate that ER stress caused by GALT-deficiency might contribute to accelerated apoptosis seen in the granulosa cells of galactosemic females, leading to premature ovarian failure [60]. Future studies using this novel, isogenic fibroblast model will elucidate other toxicity mechanisms of galactose in GALT-deficiency.

## Acknowledgments

The authors thank Dr. Louis J. Elsas, Dr. Steve Roper, Simone Sandiford, Alejandro Ocampo, Helene Klapper, and the staff of University of Miami Microarray Facility for their valuable consultation. Grant support to K.L.: NIH Grant 1R01 HD054744, American Heart Association South-East Affiliate Scientist Development Grant No. 0435267B, The Woman's Cancer Association of The University of Miami. Grant support to V.Z.S.: NIH Grant GM 060019 and American Heart Association South-East Affiliate Grant-in-Aid 0455387B.

## Appendix A. Supplementary data

Supplementary data associated with this article can be found, in the online version, at [doi:10.1016/j.ymgme.2007.06.005](https://doi.org/10.1016/j.ymgme.2007.06.005).

## References

- [1] K.J. Isselbacher et al., Congenital galactosemia, a single enzymatic block in galactose metabolism, *Science* 123 (3198) (1956) 635–636.
- [2] H.M. Kalckar, E.P. Anderson, K.J. Isselbacher, Galactosemia, a congenital defect in a nucleotide transferase, *Biochim. Biophys. Acta* 20 (1) (1956) 262–268.
- [3] S. Segal, G.T. Berry, Disorders of galactose metabolism, in: B.A. Scriver D, W. Sly, D. Valle (Eds.), *The Metabolic Basis of Inherited Diseases*, McGraw-Hill, New York, 1995, pp. 967–1000.
- [4] D. Waggoner, N.R.M. Buist, G.N. Donnell, Long-term prognosis in Galactosemia: results of a survey of 350 cases, *Journal of Inherited Metabolic Disorders* 13 (1990) 802–818.
- [5] D. Waggoner, N.R.M. Buist, Long-term complications in treated galactosemia—175 U.S. cases, *Int. Pediatr.* 8 (1993) 97–100.
- [6] P.B. Acosta, K.C. Gross, Hidden sources of galactose in the environment, *Eur. J. Pediatr.* 154 (7 Suppl. 2) (1995) S87–S92.
- [7] G.T. Berry et al., The effect of dietary fruits and vegetables on urinary galactitol excretion in galactose-1-phosphate uridylyltransferase deficiency, *J. Inher. Metab. Dis.* 16 (1) (1993) 91–100.
- [8] G.T. Berry et al., The rate of de novo galactose synthesis in patients with galactose-1-phosphate uridylyltransferase deficiency, *Mol. Genet. Metab.* 81 (1) (2004) 22–30.
- [9] G.T. Berry et al., Endogenous synthesis of galactose in normal men and patients with hereditary galactosaemia, *Lancet* 346 (8982) (1995) 1073–1074.
- [10] R. Gitzelmann, H.J. Wells, S. Segal, Galactose metabolism in a patient with hereditary galactokinase deficiency, *Eur. J. Clin. Invest.* 4 (2) (1974) 79–84.
- [11] P.J. Bhat, Galactose-1-phosphate is a regulator of inositol monophosphatase: a fact or a fiction? *Med. Hypotheses* 60 (1) (2003) 123–128.
- [12] K. Lai, L.J. Elsas, Overexpression of human UDP-glucose pyrophosphorylase rescues galactose-1-phosphate uridylyltransferase-deficient yeast, *Biochem. Biophys. Res. Commun.* 271 (2) (2000) 392–400.
- [13] K. Lai et al., GALT deficiency causes UDP-hexose deficit in human galactosemic cells, *Glycobiology* 13 (4) (2003) 285–294.
- [14] T. Slepak et al., Intracellular galactose-1-phosphate accumulation leads to environmental stress response in yeast model, *Mol. Genet. Metab.* (2005).
- [15] N.D. Leslie et al., A mouse model of galactose-1-phosphate uridylyltransferase deficiency, *Biochem. Mol. Med.* 59 (1) (1996) 7–12.
- [16] C. Ning et al., Galactose metabolism in mice with galactose-1-phosphate uridylyltransferase deficiency: sucklings and 7-week-old animals fed a high-galactose diet, *Mol. Genet. Metab.* 72 (4) (2001) 306–315.
- [17] C. Ning et al., Galactose metabolism by the mouse with galactose-1-phosphate uridylyltransferase deficiency, *Pediatr. Res.* 48 (2) (2000) 211–217.
- [18] T. Ideker et al., Integrated genomic and proteomic analyses of a systematically perturbed metabolic network, *Science* 292 (5518) (2001) 929–934.
- [19] J.K. Reichardt, S. Packman, S.L. Woo, Molecular characterization of two galactosemia mutations: correlation of mutations with highly conserved domains in galactose-1-phosphate uridylyl transferase, *Am. J. Hum. Genet.* 49 (4) (1991) 860–867.
- [20] J.L. Fridovich-Keil, S. Jinks-Robertson, A yeast expression system for human galactose-1-phosphate uridylyltransferase, *Proc. Natl. Acad. Sci. USA* 90 (2) (1993) 398–402.
- [21] K. Lai, A.C. Willis, L.J. Elsas, The biochemical role of glutamine 188 in human galactose-1-phosphate uridylyltransferase, *J. Biol. Chem.* 274 (10) (1999) 6559–6566.
- [22] A. Follenzi, L. Naldini, HIV-based vectors. Preparation and use, *Methods Mol. Med.* 69 (2002) 259–274.
- [23] A. Follenzi, L. Naldini, Generation of HIV-1 derived lentiviral vectors, *Methods Enzymol.* 346 (2002) 454–465.

- [24] V.G. Tuscher, R. Tibshirani, G. Chu, Significance analysis of microarrays applied to the ionizing radiation response, *Proc. Natl. Acad. Sci. USA* 98 (9) (2001) 5116–5121.
- [25] P. Khatra et al., Profiling gene expression using onto-express, *Genomics* 79 (2) (2002) 266–270.
- [26] S. Draghici et al., Onto-tools, the toolkit of the modern biologist: onto-express, onto-compare, onto-design and onto-translate, *Nucleic Acids Res.* 31 (13) (2003) 3775–3781.
- [27] S. Draghici et al., Global functional profiling of gene expression, *Genomics* 81 (2) (2003) 98–104.
- [28] R. Dolhofer, O.H. Wieland, Enzymatic assay of myo-inositol in serum, *J. Clin. Chem. Clin. Biochem.* 25 (10) (1987) 733–736.
- [29] J.S. Cox, P. Walter, A novel mechanism for regulating activity of a transcription factor that controls the unfolded protein response, *Cell* 87 (3) (1996) 391–404.
- [30] M. Schroder, R.J. Kaufman, ER stress and the unfolded protein response, *Mutat. Res.* 569 (1–2) (2005) 29–63.
- [31] R.J. Kaufman et al., The unfolded protein response in nutrient sensing and differentiation, *Nat. Rev. Mol. Cell Biol.* 3 (6) (2002) 411–421.
- [32] M. Schroder, R.J. Kaufman, The mammalian unfolded protein response, *Annu. Rev. Biochem.* 74 (2005) 739–789.
- [33] N. Hosokawa et al., EDEM accelerates ERAD by preventing aberrant dimer formation of misfolded  $\alpha$ 1-antitrypsin, *Genes Cells* 11 (5) (2006) 465–476.
- [34] K.K. Eriksson et al., EDEM contributes to maintenance of protein folding efficiency and secretory capacity, *J. Biol. Chem.* 279 (43) (2004) 44600–44605.
- [35] N. Hosokawa, ER quality control and ERAD: EDEM accelerates glycoprotein ERAD, *Tanpakushitsu Kakusan Koso* 49 (Suppl. 7) (2004) 984–987.
- [36] D.A. Applegarth et al., Study of a family with Los Angeles, Duarte, and classical galactosemia variants of galactose-1-phosphate uridyl transferase, *Biochem. Med.* 15 (2) (1976) 206–211.
- [37] E. Little et al., Induction of glucose-regulated protein (glucose-regulated protein 78/BiP and glucose-regulated protein 94) and heat shock protein 70 transcripts in the immature rat brain following status epilepticus, *Neuroscience* 75 (1) (1996) 209–219.
- [38] J.B. Tillman et al., Structure and regulation of the mouse GRP78 (BiP) promoter by glucose and calcium ionophore, *Gene* 158 (2) (1995) 225–229.
- [39] M. Hashii, Y. Nozawa, H. Higashida, Bradykinin-induced cytosolic  $\text{Ca}^{2+}$  oscillations and inositol tetrakisphosphate-induced  $\text{Ca}^{2+}$  influx in voltage-clamped ras-transformed NIH/3T3 fibroblasts, *J. Biol. Chem.* 268 (26) (1993) 19403–19410.
- [40] R. Parthasarathy, L. Parthasarathy, R. Vadnal, Brain inositol monophosphatase identified as a galactose 1-phosphatase, *Brain Res.* 778 (1) (1997) 99–106.
- [41] L.J. Elsas et al., Galactosemia: a strategy to identify new biochemical phenotypes and molecular genotypes, *Am. J. Hum. Genet.* 56 (3) (1995) 630–639.
- [42] J.E. Flach, J.K. Reichardt, L.J. Elsas, 2nd, Sequence of a cDNA encoding human galactose-1-phosphate uridyl transferase, *Mol. Biol. Med.* 7 (4) (1990) 365–369.
- [43] A.M. Bosch et al., Living with classical galactosemia: health-related quality of life consequences, *Pediatrics* 113 (5) (2004) e423–e428.
- [44] R. Gitzelmann, Galactose-1-phosphate in the pathophysiology of galactosemia, *Eur. J. Pediatr.* 154 (7 Suppl. 2) (1995) S45–S49.
- [45] R. Gitzelmann, Formation of galactose-1-phosphate from uridine diphosphate galactose in erythrocytes from patients with galactosemia, *Pediatr. Res.* 3 (4) (1969) 279–286.
- [46] R. Gitzelmann, H.C. Curtius, I. Schneller, Galactitol and galactose-1-phosphate in the lens of a galactosemic infant, *Exp. Eye Res.* 6 (1) (1967) 1–3.
- [47] R. Gitzelmann, Letter: Additional findings in galactokinase deficiency, *J. Pediatr.* 87 (6 Pt. 1) (1975) 1007–1008.
- [48] R. Gitzelmann, Deficiency of erythrocyte galactokinase in a patient with galactose diabetes, *Lancet* 2 (7414) (1965) 670–671.
- [49] T. Slepak et al., Intracellular galactose-1-phosphate accumulation leads to environmental stress response in yeast model, *Mol. Genet. Metab.* 86 (3) (2005) 360–371.
- [50] L.W. Ruddock, M. Molinari, N-glycan processing in ER quality control, *J. Cell Sci.* 119 (Pt. 21) (2006) 4373–4380.
- [51] J. Charlwood et al., Defective galactosylation of serum transferrin in galactosemia, *Glycobiology* 8 (4) (1998) 351–357.
- [52] J.A. Dobbie, J.B. Holton, J.R. Clamp, Defective galactosylation of proteins in cultured skin fibroblasts from galactosaemic patients, *Ann. Clin. Biochem.* 27 (Pt. 3) (1990) 274–275.
- [53] J. Jaeken, J. Kint, L. Spaepen, Serum lysosomal enzyme abnormalities in galactosaemia, *Lancet* 340 (8833) (1992) 1472–1473.
- [54] K.S. Ornstein et al., Abnormal galactosylation of complex carbohydrates in cultured fibroblasts from patients with galactose-1-phosphate uridyltransferase deficiency, *Pediatr. Res.* 31 (5) (1992) 508–511.
- [55] L.L. Prestoz et al., Altered follicle stimulating hormone isoforms in female galactosaemia patients, *Eur. J. Pediatr.* 156 (2) (1997) 116–120.
- [56] K.J. Travers et al., Functional and genomic analyses reveal an essential coordination between the unfolded protein response and ER-associated degradation, *Cell* 101 (3) (2000) 249–258.
- [57] J.P. Navarro-Avino, J.M. Belles, R. Serrano, Yeast inositol mono- and trisphosphate levels are modulated by inositol monophosphatase activity and nutrients, *Biochem. Biophys. Res. Commun.* 302 (1) (2003) 41–45.
- [58] S. Sarkar et al., Lithium induces autophagy by inhibiting inositol monophosphatase, *J. Cell Biol.* 170 (7) (2005) 1101–1111.
- [59] M.J. Berridge, C.P. Downes, M.R. Hanley, Neural and developmental actions of lithium: a unifying hypothesis, *Cell* 59 (3) (1989) 411–419.
- [60] K.W. Lai et al., Inhibitor of apoptosis proteins and ovarian dysfunction in galactosemic rats, *Cell Tissue Res.* 311 (3) (2003) 417–425.